Available online at www.sciencedirect.com
SCIENCE DIRECT®
Analytical Biochemistry 344 (2005) 257–265
ANALYTICAL BIOCHEMISTRY
www.elsevier.com/locate/yabio

Sensitivity comparison of real-time PCR probe designs on a model DNA plasmid

L. Wang [a,*], J.R. Blasic Jr. [a], M.J. Holden [a], R. Pires [b]

[a] *Biotechnology Division, National Institute of Standards and Technology, Gaithersburg, MD 20899, USA*
[b] *Invitrogen Corporation, Frederick, MD 21704, USA*

Received 5 May 2005
Available online 25 July 2005

Abstract

We investigated three probe design strategies used in quantitative polymerase chain reaction (PCR) for sensitivity in detection of the PCR amplicon. A plasmid with a 120-bp insert served as the DNA template. The probes were TaqMan, conventional molecular beacon (MB), and shared-stem molecular beacon (ATssMB and GCssMB). A shared-stem beacon probe combines the properties of a TaqMan probe and a conventional molecular beacon. It was found that the overall sensitivities for the four PCR probes are in the order of MB > ATssMB > GCssMB > TaqMan. The fluorescence quantum yield measurements indicate that incomplete or partial enzymatic cleavage catalyzed by *Taq* polymerase is the likely cause of the low sensitivities of two shared-stem beacons when compared with the conventional beacon probe. A high-fluorescence background associated with the current TaqMan probe sequence contributes to the relatively low detection sensitivity and signal-to-background ratio. The study points out that the nucleotide environment surrounding the reporting fluorophore can strongly affect the probe performance in real-time PCR.
Published by Elsevier Inc.

Keywords: Quantitative real-time PCR; Probe design; TaqMan; Molecular beacon; Shared-stem molecular beacon; DNA plasmid; Detection sensitivity; Signal-to-background ratio; 5′ Exonuclease activity; Fluorescence quantum yield; Melting temperature

Nucleic acid detection and quantification play important roles in many areas, including cancer diagnostics, drug discovery, and biotechnology-derived crop identification and quantification. Often the quantities of DNA and RNA are too small for direct measurement, and so amplification of the target by the polymerase chain reaction (PCR)[1] is required. The need for quantification of genetic elements is the driving force for the current development of quantitative PCR methods. Because of high sensitivity and a large dynamic range, fluorescence detection methods are used in real-time PCR [1,2]. Commonly used formats include fluorescent dyes (e.g., SYBR Green I), which bind to the minor groove of the DNA double helix [3,4], and oligonucleotide probes, which are complementary to a portion of the amplified target. These oligonucleotide probes contain both a fluorophore and a quencher that interact through a fluorescence resonance energy transfer mechanism [5–9]. When compared with the DNA binding dyes, fluorophores linked to oligonucleotides offer higher sequence specificity and are less susceptible to contamination, such as primer–dimer formation in the case of SYBR Green I [10,11], and are relatively easier for the detection of single nucleotide polymorphisms [7,12,13].

Fluorescence resonance energy transfer is the underlying mechanism for various real-time PCR methods employing a variety of probe design tactics, including

* Corresponding author. Fax: +1 301 975 5449.
E-mail address: lili.wang@nist.gov (L. Wang)

[1] *Abbreviations used:* PCR, polymerase chain reaction; MB, conventional molecular beacon; AtssMB and GCssMB, shared-stem molecular beacon; TAMRA, 5-carboxytetramethylrhodamine CPG; HPLC, high-performance liquid chromatography; MALDI–TOF, matrix-assisted laser desorption ionization time-of-flight; SRM, Standard Reference Material; SVP, snake venom phosphodiesterase; BSPD, bovine spleen phosphodiesterase.

0003-2697/$ - see front matter. Published by Elsevier Inc.
doi:10.1016/j.ab.2005.06.038

TaqMan probes [8], molecular beacons [14,15], and hybridization probes [16]. Because of probe design, molecular beacons give low initial fluorescence background. The stem structure of the molecular beacons warrants efficient fluorescence quenching by the proximal quencher. In comparison, TaqMan probes give much higher background signals in that the intramolecular separation distance between a donor and an acceptor in the unhybridized state results in only partial quenching. The amount of resonance energy transfer is considerably lower than that in the case of molecular beacons.

More recently, a variety of new molecular beacon designs have been explored for higher affinity binding with targets though lower discrimination between closely related targets. These probes interact with a target sequence along the loop length and throughout one stem [17] or both stem regions [18] to increase effective hybridization length with the target. To eliminate nonspecific binding of stems with a target, Browne designed sequence-specific, self-reporting hairpin inversion beacon probes to improve specificity of hybridization [19]. In addition, Kong et al. reported shared-stem molecular beacon probes that combined properties of TaqMan probes and conventional molecular beacons [20]. The authors have shown that the signal-to-background ratios are superior to those of conventional molecular beacons using this probe design strategy. Understandably, fluorescence from a fluorophore cleaved from a nucleotide probe ought to be greater than fluorescence from a fluorophore separated from a quencher by approximately 20 nucleic bases as in the case of a conventional molecular beacon.

In the current study, a 120-bp template was designed and inserted into a plasmid. There was a desire to have a template that was suitable for evaluation of several probe types but that resembled no known gene so as to avoid contamination of PCRs that measured actual genes. Various probe types were employed: TaqMan probe, conventional molecular beacon (MB), and shared-stem molecular beacon (ATssMB and GCssMB). We compared their signal-to-background ratios and sensitivities with respect to the same amplicon. The investigation is in support of our effort to develop model DNA reference materials for standardizing real-time PCR instruments and protocols.

Materials and methods

Preparation of various PCR probes and model DNA plasmid

Probes were designed to have a melting temperature with the complementary strands and of the stem structure of the beacons between 61 and 63 °C (7–10 °C above the annealing temperature of 55 °C) and to have no other internal secondary structures above 50 °C. The melting temperatures of probe to target and of intramolecular stem were determined by the nearest neighbor model and by Mfold Web server (version 3.1) [21]. 5′-Fluorescein phosphoramidite, 5-carboxytetramethylrhodamine CPG (TAMRA), and 3′-dabsyl CPG were obtained from Glen Research (Sterling, VA, USA).[2] The oligonucleotide PCR probes were synthesized on a 96-well DNA synthesizer using standard phosphoramidite chemistry. Oligos containing 3′ TAMRA were cleaved from the CPG and deprotected using a *tert*-butylamine/methanol/water (1:1:2) mixture at 85 °C for 2 h [22]. The final products were purified by high-performance liquid chromatography (HPLC) and verified by matrix-assisted laser desorption ionization time-of-flight (MALDI–TOF) mass spectrometry using either a Biflex III (Bruker, Billerica, MA, USA) or a Voyager DE Pro (PerSeptive Biosystems, Framingham, MA, USA). A model DNA construct (120 bp) was assembled from six overlapping fragments of DNA ranging in size from 26 to 43 bp via PCR (MJ Research Mini Cycler) [23]. The assembled sequence was then cloned into PCRscript Cam plasmid vector from Stratagene (La Jolla, CA, USA) and transformed into XL10 Gold cells (Stratagene). The plasmid (3519 bp in length) was isolated from culture by alkaline lysis and purified on a CsCl gradient. The sequences of the primers, the real-time PCR amplicon, and various PCR probes are given in Table 1, and their lengths and location with respect to the amplicon are shown later in Fig. 1. In addition, two oligonucleotides—TaqssMB and CompMB—are shown in the same table and used for quantum yield measurements. All of the concentrations were determined based on absorbance measurements at 260 nm and extinction coefficients given in [24]. A recent BLAST search [25] indicated that several fragments of 19–22 bp of the template had homologies to sequences found in the *Homo sapiens*, *Mus musculum*, *Oryze sativa*, *Legionella pneuophila*, *Silicibacter pomeroyi*, *Ustilago maydis*, and *Gibberella zeae* genomes. None of these fragments precisely overlaps any of the primers or probes used in this study.

Real-time PCR protocols

For PCR measurements, the fluorescence signal was detected by the green fluorescence channel (530 nm) of the LightCycler from Roche Diagnostics (Indianapolis, IN, USA) at the end of the annealing step (55 °C) using the following protocols: 95 °C for 10 min for enzyme activation due to the use of LightCycler FastStart DNA

[2] Certain commercial equipment, instruments, and materials are identified in this article to specify the experimental procedure adequately. In no case does such identification imply recommendation or endorsement by the National Institute of Standards and Technology, nor does it imply that the equipment, instruments, or materials are necessarily the best available for the purpose.

Table 1
Oligonucleotide sequences

Name	Fluorophore	Sequence
Amplicon	None	5′-AGGACGTGGACCAGAGATCGA ATGACCATCGTGTGCTGACTCCAGAGGT TGCAGTCA GCGAGTGCATCAGGTGTTGAAGCCTGATCCCTGTTCCGAAGTACCTATCGTCGAGCGGTC TGT-3′
Forward primer	None	5′-ACAGACCGCTCGACGATAGG-3′
Reverse primer	None	5′-AGGACGTGGACCAGAGATCG-3′
TaqMan	5′-Fluorescein 3′-Rhodamine	5′-ACTTCGGAACAGGGATCAGGCTACA-3′
ATssMB	5′-Fluorescein 3′-Dabsyl	5′-ACTTCGGAACAGGGATCAGGCTACAccgaagt-3′
GCssMB	5′-Fluorescein 3′-Dabsyl	5′-CGGAACAGGGATCAGGCTACAACAgttccg-3′
MB	5′-Fluorescein 3′-Dabsyl	5′-ccgccCTCTGGAGTCAGCACACGATGGTCAggcgg-3′
GC-TaqMan	5′-Fluorescein 3′-Rhodamine	5′-CGGAACAGGGATCAGGCTACAACAC-3′
TaqssMB	None	5′-AGGTGTTGTAGCCTGATCCCTGTTCCGAAGTACCTAT-3′
CompMB	None	5′-ATCGAATGAC CATC GTGTG CTGACTCCAGAGGT TGCAGTCAGCGAGTGCATCAGGT GTTGTAG-3′

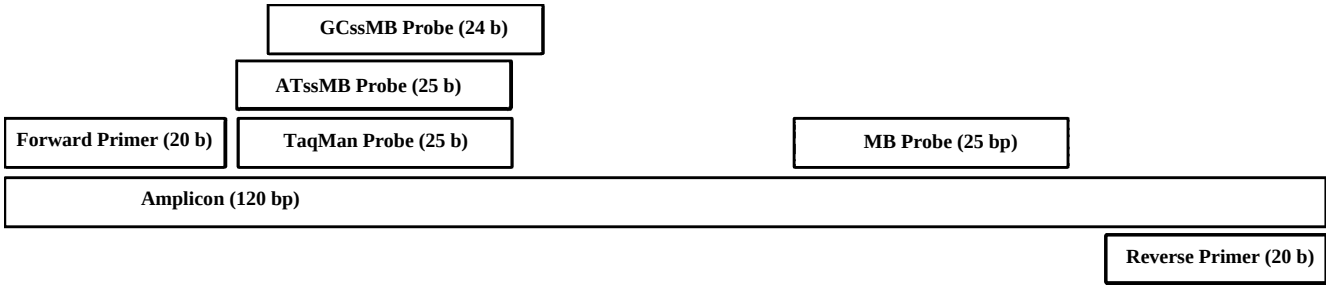

Fig. 1. Positions and lengths of various real-time PCR probes and forward and reverse primers with respect to the amplified region of the model DNA plasmid. The lengths include only the regions involved in hybridization.

Master Hybridization Probes from Roche; for the TaqMan and shared-stem molecular beacon probes, 95 °C for 15 s, then decreasing the temperature to 55 °C and incubation for 30 s, repeating the cycle; for the molecular beacon probe, 95 °C for 10 s, then decreasing the temperature to 55 °C for 10 s, followed by increasing the temperature to 72 °C and incubation for 30 s at 72 °C, restarting the cycle. The PCRs were optimized first by magnesium titration to determine the optimal magnesium concentration, followed by a temperature gradient to determine the best annealing temperature. Primer and probe concentrations were then optimized experimentally. The optimized reaction conditions were 500 nM forward and reverse primers, 1 μM probe, and 2 mM magnesium chloride for all reactions except the conventional molecular beacon probe, with which 3 mM magnesium chloride was employed. PCR amplification was carried out for 45 cycles for all probe designs.

5′ Exonuclease activity measurements

Because fluorescence signal on PCR amplification is critically dependent on 5′ exonuclease cleavage for both TaqMan and shared-stem molecular beacon probes, we designed experiments to verify the effectiveness of the exonuclease cleavage. Samples with probe included, with no probe, and with only probe and buffer present were run through 45 cycles of PCR amplification using the LightCycler. On completion of the thermocycling protocol, the reactions containing cycled probe only were added to the samples that had cycled with no probe. These served as the control for the measurements. A portion of the reaction mixture (15 μl) was withdrawn from each pool. The remaining sample was then filtered through a Microcon YM-3 (molecular weight cutoff of 3000 Da, 10 single-stranded nucleotides) centrifugal filter device from Millipore (Bedford, MA, USA) at 13,000*g* for 30 min. A 15-μl portion was withdrawn from the filtrate. These samples, along with those without filtration, were loaded back into LightCycler capillaries and heated up to 95 °C for 2 s, followed by fluorescence reading at 55 °C using the real-time fluorometer function of the LightCycler.

Fluorescence quantum yield measurements

The steady-state fluorescence measurements were carried out using an SLM 8000 spectrofluorometer from Jobin Yvon (Edison, NJ, USA). The fluorescence spectra

were recorded under the "magic angle" condition with the excitation wavelength of 480 nm for fluorescein. The slits for the excitation and emission monochromators both were set at 4 nm. Relative fluorescence quantum yields were determined with respect to a fluorescein standard (NIST Standard Reference Material (SRM) 1932, Gaithersburg, MD, USA), which was diluted to 0.5 μM in 0.1 M borate buffer (pH 9.1). Under these conditions, the fluorescein standard gives a quantum yield of 0.93 that is equivalent to the value reported in 0.01 M NaOH [26]. To get accurate absorbance of fluorescein at 480 nm, dG-dabsyl, a rhodamine-labeled oligonucleotide, and a fluorescein-labeled oligonucleotide were used to derive the absorbance of fluorescein only at 480 nm using Mathcad 2001 software from MathSoft (Cambridge, MA, USA). The quantum yields were obtained at room temperature and calculated using the equation given by Turner [27]. In addition, two enzymes—snake venom phosphodiesterase (SVP) and bovine spleen phosphodiesterase (BSPD)—were used to verify the results of enzymatic digestion. Both enzymes are products from Invitrogen (Carlsbad, CA, USA).

Sensitivity measurements

To test the sensitivity of various PCR probe designs, the model plasmid was preamplified for 45 cycles using the LightCycler without a probe and fluorescence detection. The amplified DNA construct was then diluted to 1×10^{13} copies per microliter. Each probe was then added, along with other fresh reagents, to a 10-fold dilution series of the amplified construct solution (1×10^{13}/μl) and run in triplicate. These samples went through two cycles of amplification, along with a "no DNA control," to account for the difference in measurement from cycle to cycle. The fluorescence signal of the first cycle was subtracted from the signal of the second cycle to obtain the signal increase resulting from one round of amplification with the respective amount of starting material. In this manner, we attempted to recreate the conditions during a PCR with well-defined quantities of amplified product. Data were averaged and plotted with the background subtracted.

Results and discussion

Fig. 1 shows the positions of the four real-time PCR probes with respect to the PCR amplicon. The probes used in the study were a TaqMan probe, two shared-stem molecular beacons, and a conventional molecular beacon. With the use of both TaqMan and shared-stem molecular beacon probes, signal amplification relies on hybridization with the amplicon and hydrolysis of the probe by the 5′-exonuclease activity of *Taq* DNA polymerase (55 °C); therefore, these probes were placed close to the forward primer to enhance hydrolysis efficiency. For the molecular beacon probe, the final signal depends on the amplicon concentration and hybridization efficiency with the amplicon. In this case, the molecular beacon probe is displaced from the target by *Taq* DNA polymerase (72 °C). The location of the probe on the target was positioned some distance from the primer. Because of these differences, the thermal cycling profiles using these probes were different, as detailed in Materials and methods.

Fig. 2A shows fluorescence intensities after completion of PCR (gray columns) for the four PCR probes. The black columns in the same figure show the initial fluorescence backgrounds averaged over the first five PCR cycles. To account for possibly unequal concentrations of probes and differences in fluorescence quantum yields of fluorescein in each case, the signal-to-background ratios were calculated and are displayed in Fig. 2B for the comparison of the four probes. The ratio trails in the following order: MB > GCssMB > ATssMB > TaqMan. A conventional molecular beacon probe, by design, gives a low-fluorescence background when compared with a TaqMan probe in that fluorescence from the fluorophore is highly quenched by the adjacent quencher, as seen in Fig. 2A (black columns). In addition, the guanine bases in the stem portion of the beacon quench the fluorescence of the fluorophore. The amount of fluorescence quenching is gener-

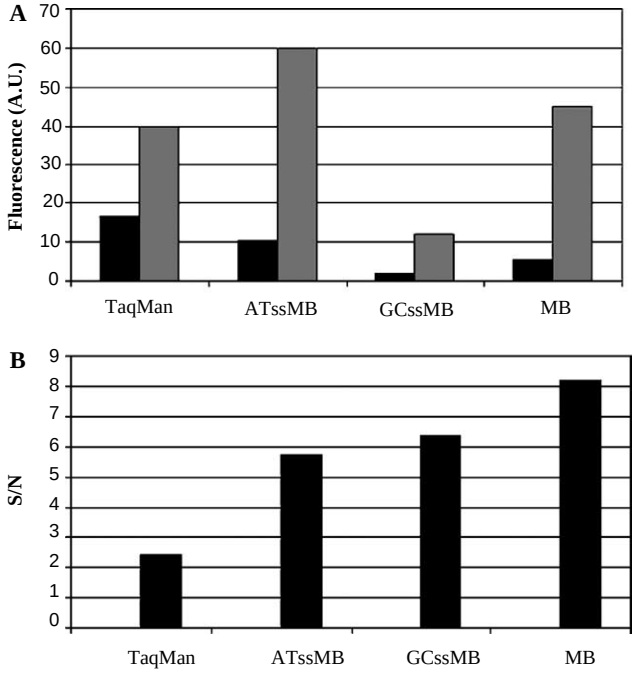

Fig. 2. (A) Fluorescence signal after completion of PCR (gray columns) for various real-time PCR probes. The black columns show the initial fluorescence backgrounds averaged over the first five PCR cycles. AU, arbitrary units. (B) Signal-to-background ratios (S/N) obtained using the data given in (A) for the four real-time PCR probes.

ally proportional to the number of nearby guanine bases (in the neighborhood of 5 or 6 bases) [28–30]. Based on these principles, we expected the fluorescence backgrounds of the three molecular beacon probes to be in the order of MB < GCssMB < ATssMB. The fluorescence background from GCssMB (Fig. 2A) is surprisingly the lowest among the three beacon probes used in the study. On the other hand, with the use of TaqMan, ATssMB, and GCssMB probes, the signal enhancement is critically dependent on hydrolysis activity of the polymerase during PCR. The final signals after PCR should be comparable among the three probes, yet they are very different (Fig. 2A). The signal from ATssMB is the highest, whereas the signal from GCssMB is the lowest. By design, the GCssMB probe should give a better signal-to-background ratio than the ATssMB probe if the former is hydrolyzed completely during the PCR and obeys the quenching rule by the number of guanine bases in the stem portion.

We developed a method for verifying the effectiveness of the exonuclease cleavage of various PCR probes during the PCR cycling protocol, as detailed in Materials and methods. Fig. 3 compares fluorescence signals of samples after PCR (black columns), the post-PCR filtrates using Microcon YM-3 centrifugal filter devices (gray columns), and the control samples (striped columns). Controls consisted of combined filtrates of a post-PCR solution with no probe present during PCR and a second solution of probe that had gone through the same number of thermocycles in the absence of target. For TaqMan and two shared-stem beacon probes, the signals from the filtrates were about the same as the signals after PCR, inferring that the signals were from lysed probes (equal to or smaller than 10 single-stranded nucleotides in size). As expected, the MB probe was not lysed during PCR and was retained by the filter; hence, the fluorescence signal on completion of PCR was much higher than that of the filtrate.

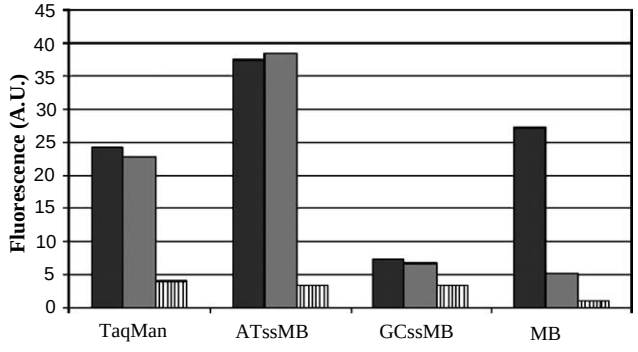

Fig. 3. Fluorescence signal comparison among samples after PCR (black columns), the same volume post-PCR filtrate using Microcon YM-3 centrifugal filter devices (gray columns), and the controls (striped columns) consisting of combined filtrates of a post-PCR solution with no probe present during PCR and a second solution of probe that had gone through the same number of thermocycles in the absence of target (see Materials and methods). AU, arbitrary units.

The fluorescence quantum yields of the post-PCR filtrates were measured and are given in Table 2 for TaqMan, ATssMB, and GCssMB probes. The yields of TaqMan and ATssMB probes are relatively close. Although they are lower than expected, it is evident that hydrolysis cleavage takes place during PCR. The yield of GCssMB is, nonetheless, much lower than the yields of the other two probes. When a GCssMB probe is hybridized to the amplicon, its location is shifted from the primer by 4 more nucleic acid bases than are ATssMB and TaqMan probes. We synthesized a control probe, GC-TaqMan, which has the identical sequence at the 5′ end as the GCssMB probe and which has no 3′ end stem sequence to verify whether the hydrolysis reaction indeed takes place during real-time PCR. The quantum yield determined for the post-PCR filtrate is 0.59 using GC-TaqMan as the probe. This suggests that the polymerase can effectively cleave the probe and result in an increase of fluorescence signal due to physical separation of the fluorophore from the quencher.

Table 2
Relative fluorescence quantum yields determined for control samples and filtrates after PCR

Sample	Quantum yield[a]
Control	
dC-fluorescein	0.81
dA-fluorescein	0.81
dCG-fluorescein	0.20
dCGG-fluorescein	0.23
dCGGA-fluorescein	0.42
Probe and duplex with complementary strand[b]	
TaqMan	0.19
TaqMan/TaqssMB	0.65
ATssMB	0.081
ATssMB/TaqssMB	0.78
GCssMB	0.028
GCssMB/TaqssMB	0.43
MB	0.050
MB/CompMB	0.64
GC-TaqMan	0.11
GC-TaqMan/TaqssMB	0.49
Samples after enzymatic digestion	
GCssMB + SVP	0.75
GCssMB + BSPD	0.77
GCssMB + SVP + BSPD	0.71
Post-PCR filtrate	
TaqMan	0.38
ATssMB	0.47
GCssMB	0.12
GC-TaqMan	0.59

[a] Quantum yields were averaged over several experimental repeats with standard deviations of less than 5% for the control, probe alone, and duplexes with the complementary strand and samples after enzymatic digestion, and with standard deviations of ⩽20% for post-PCR filtrates.

[b] The samples in 20 mM Tris–HCl (pH 8.4), 50 mM KCl, and 2 mM $MgCl_2$ went through the following protocol: 25 °C for 30 s, 95 °C for 2 min, then decreasing the temperature to 25 °C at the rate of 0.2 °C/s and incubating for 8 min at 25 °C.

Considering that the polymerase was able to cleave the control sequence GC-TaqMan, we questioned whether GCssMB was fully opened and able to hybridize to the amplicon, as expected in PCR. The melting curves and their first negative derivatives over the temperature range of 30–95 °C are shown in Fig. 4 for three beacon probes and their duplexes with the complementary strands. The obtained melting temperatures for both GCssMB (60.5 °C) and ATssMB (58.8 °C) are similar and 8–10 °C lower than those for their duplexes with the complementary target (TaqssMB), that is, 68.4 and 69.0 °C for GCssMB duplex and ATssMB duplex, respectively. These temperatures are generally consistent with the probe design strategies. The results imply that GCssMB should behave similarly to ATssMB in real-time PCR and should be able to hybridize to the complementary strand. The melting temperature for the MB probe is slightly higher than the melting temperatures for the two shared-stem molecular beacons (62.1 °C), consistent with the higher GC content in the stem portion of MB. Taking into account that the concentrations of the probes were kept approximately the same for the measurements, the fluorescence signals from the GCssMB probe and its duplex with the target are significantly lower than the others.

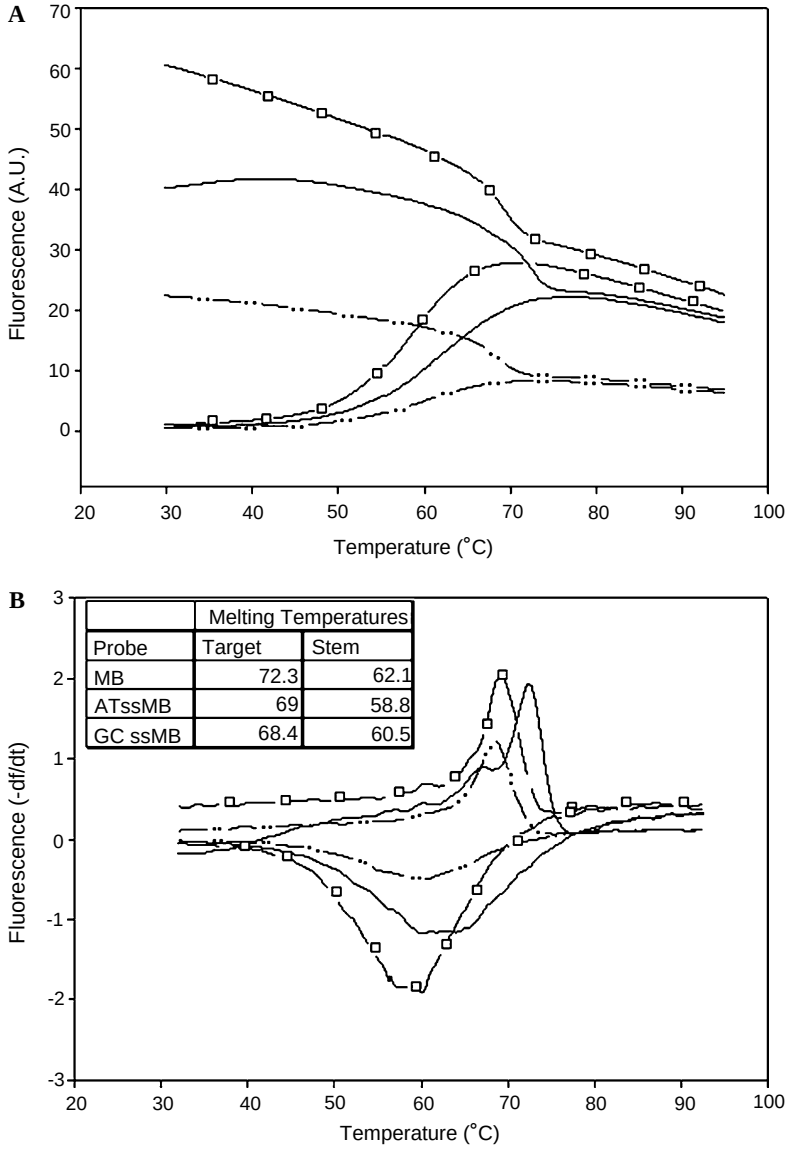

Fig. 4. Melting curves (A) and first negative derivatives over the temperature (B) for three beacon probes and their duplexes with the complementary oligonucleotides (TaqssMB for two shared-stem beacons and CompMB for the conventional molecular beacon) using the LightCycler: -□-, AtssMB; —, MB; -···, GCssMB. The probe alone or the mixture of the probe and the complementary target in 20 mM Tris–HCl (pH 8.4), 50 mM KCl, and 2 mM $MgCl_2$ went through the following protocol: 95 °C for 30 s, then decreasing to 30 °C at the rate of 0.2 °C/s and holding at 30 °C for 30 s, followed by a slow ramp (0.1 °C/s) to 95 °C with continuous fluorescence monitoring. The (B) inset lists the melting temperatures obtained by taking the peak reading of the first negative derivative over the temperature. AU, arbitrary units.

We further questioned whether C-linked fluorescein resulting from the complete hydrolysis of the GCssMB probe would be quenched. Both dC-fluorescein and dA-fluorescein were synthesized to serve as controls. Their fluorescence quantum yields measured against the reference standard are the same (0.81) and are given in Table 2. We measured the quantum yields of GCssMB alone in Tris buffer (pH 8.4) and the GCssMB probe digested by two different enzymes either separately or jointly (Table 2). Enzymatic digestion by SVP starts from the 5′ end of the nucleotides, and digestion catalyzed by BSPD originates from the 3′ end of the nucleotides. The yields for digested GCssMB are close to each other and above 0.70, inferring that fully cleaved GCssMB should fluoresce strongly. Three additional control samples—dCG-fluorescein, dCGG-fluorescein, and dCGGA-fluorescein—were made to show the likely outcomes of partial hydrolyses of GCssMB serving as the probe in PCR. The fluorescence quantum yields of these controls are given in Table 2. The yields of dCG-fluorescein (0.20) and dCGG-fluorescein (0.23) are about four times lower than the yield of dC-fluorescein (0.81), and the yield of dCGGA-fluorescein (0.42) is approximately half that of dC-fluorescein. These results point out that low fluorescence signal after PCR using GCssMB as the probe is most likely due to partial hydrolysis of the probe. Although the quantum yield determined for GCssMB after PCR (0.12) is much lower than anticipated, it is more than four times higher than that of GCssMB in the stem-loop state (0.028). When a GCssMB probe was hybridized to its complementary oligonucleotide, TaqssMB, the quantum yield of the formed duplex (GCssMB/TaqssMB) was measured to be 0.43. This yield is much higher than that after PCR (0.12). The measured yield (0.43) in the duplex form is comparable to that of the duplex GC-TaqMan/TaqssMB (0.49) (Table 2) due to the same microenvironment fluorophores experienced in both cases. Interestingly, the quantum yields of the four PCR probes increase in the order of GCssMB < MB < ATssMB

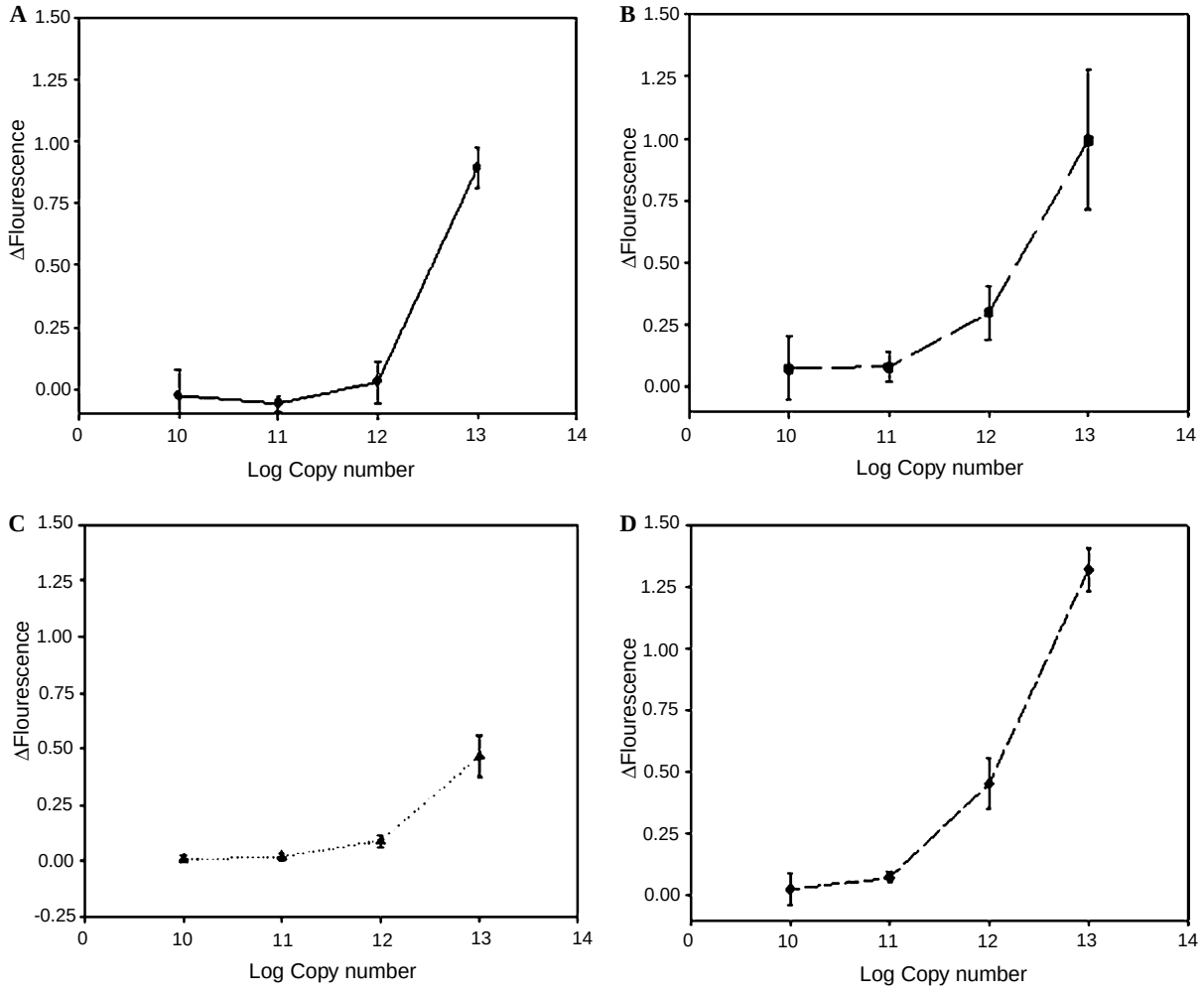

Fig. 5. Differences in fluorescence signals between second and first PCR amplification cycles as a function of the concentrations (copy numbers) of the starting amplicons for TaqMan (A), AtssMB (B), GCssMB (C), and MB (D). The plots include the standard deviations from nine replicates for each concentration.

< TaqMan. The trend is the same, as shown in Fig. 2A (black columns). It is also worth noting that the control probe (GC-TaqMan) would be a better probe than TaqMan when comparing the quantum yields of probes alone and post-PCR filtrates (Table 2). The fluorescence signal increases fivefold after PCR for GC-TaqMan and approximately twofold for TaqMan. The results suggest that one could use surrounding nucleotide sequences to improve assay sensitivities when designing PCR probes.

To compare the sensitivities of various PCR probes, we prepared a 10-fold dilution series of the preamplified DNA construct (1×10^{13}/μl). With the same amount of starting material, the signal difference between the second and first PCR amplification cycles is likely to show the sensitivity of the probe. Fig. 5 displays differences in measured fluorescence signals as a function of the concentration (logarithmic copy number) of the starting construct for TaqMan (panel A), ATssMB (panel B), GCssMB (panel C), and MB (panel D). With a starting copy number of 1×10^{12} per microliter, the signal difference between the second and first amplification cycles is distinguishable from that of less starting material, for instance, 1×10^{11} copies per microliter using MB, ATssMB, and GCssMB probes. Because of intrinsic high-fluorescence background associated with the TaqMan probe, the signal difference was not significant enough to differentiate the starting material from 1×10^{12} to 1×10^{11} copies per microliter. The overall sensitivities for the four probe types are in the order of MB > ATssMB > GCssMB > TaqMan. The sensitivity result is generally consistent with that of the signal-to-background ratio shown in Fig. 2B and the C_t values obtained from one to six orders of magnitude dilutions of the plasmid. The molecular beacon probe, MB, gives a low initial background and a much higher fluorescence signal when hybridized to the complementary target. The increase in fluorescence signal results from decreased quenching by the energy acceptor, dabsyl. The shared-stem beacon probes also give low-fluorescence background; nonetheless, the fluorescence enhancement during PCR depends on the efficiency of enzymatic hydrolysis of the probes. Our original hypothesis, namely that a shared-stem molecular beacon would be a better probe than a conventional beacon probe due to the strong initial quenching and lyses of the fluorophore from the probe to give a large final signal, assumes 100% cleavage efficiency (a single nucleic base conjugated with a fluorescein) and no interference from proteins and nucleotides. It is apparent from the quantum yield measurements (Table 2) that the efficiency of enzymatic cleavage of the probes can vary from one probe to another and that final products may be various small-length nucleotides. Between the two shared-stem beacon probes, we observed a low-fluorescence signal of GCssMB after PCR, although the performances of the two probes were very similar. We do not see superior signal-to-background ratios with the two shared-stem beacon probes in this study, and we do not compare our results with those reported by Kong et al. [20] due to very different sequences (microenvironments surrounding the fluorophore) used in PCR measurements.

Conclusions

Quantitative real-time PCR has been accepted as the standard method for nucleic acid detection and quantification. Sequence-specific probes for such detection and quantification are the cornerstones of the genomic revolution and of molecular diagnostics. Hence, it is important not only to continuously explore new probe design tactics but also to investigate existing probe designs and provide guidelines for obtaining the most sensitive probes for the desired applications. In the current study, a model DNA plasmid that contains a 120-bp sequence serving as the amplicon of real-time PCR was constructed to investigate various probe design strategies. Three different probe designs were compared for detection sensitivity of amplifying the 120-bp sequence: a TaqMan, a conventional molecular beacon, and two shared-stem molecular beacons. It was found that the conventional molecular beacon showed the highest sensitivity and signal-to-background ratio, whereas the TaqMan probe displayed the lowest sensitivity and signal-to-background ratio for amplifying the 120-bp sequence region of the model plasmid. The sensitivities of the two shared-stem molecular beacons were similar but slightly lower than the sensitivity of the conventional beacon probe. The fluorescence quantum yield measurements reveal that an incomplete enzymatic hydrolysis associated with the TaqMan probe design tactic is the likely cause of the measured sensitivity of the shared-stem beacon probe, GCssMB. With a relatively clean preparation of DNA for real-time PCR, it is essential to design a probe with relatively low-fluorescence background to obtain high-detection sensitivity. In the case of TaqMan and GC-TaqMan probes, for instance, moving the probe sequence around in the nearby region and using the local microenvironment of the fluorophore can reduce the fluorescence background and improve the signal-to-background ratio of PCR (GC-TaqMan would perform better than TaqMan). The investigation is in support of our effort to develop model DNA reference materials for standardizing real-time PCR instruments and protocols. Ultimately, the model DNA plasmid can be used to calibrate various real-time PCR instruments with numerous probe design strategies.

Acknowledgment

The authors are indebted to P. Vallone for his critical reading and discussion of the manuscript.

References

[1] S. Meuer, C.T. Wittwer, K. Nakagawara (Eds.), Rapid Cycle Real-Time PCR: Methods and Applications, Springer, Berlin, 1999.
[2] C.T. Wittwer, M.G. Herrmann, A.A. Moss, R.P. Rasmussen, Continuous fluorescence monitoring of rapid cycle DNA amplification, BioTechniques 22 (1997) 130–138.
[3] M. Nakao, J.W.G. Janssen, T. Flohr, C.R. Bartram, Rapid and reliable quantification of minimal residual disease in acute lymphoblastic leukemia using rearranged immunoglobulin and T-cell receptor Loci by LightCycler technology, Cancer Res. 60 (2000) 3281–3289.
[4] A.K. Dhar, M.M. Roux, K.R. Klimpel, Detection and quantification of infectious hypodermal and hematopoietic necrosis virus and white spot virus in shrimp using real-time quantitative PCR and SYBR Green chemistry, J. Clin. Microbiol. 39 (2001) 2835–2845.
[5] S. Tyagi, F.R. Kramer, Molecular beacons: probes that fluoresce upon hybridization, Nat. Biotechnol. 14 (1996) 303–308.
[6] K. Szuhai, E. Sandhaus, S.M. Kolkman-Uljee, M. Lemaitre, J.C. Truffert, R.W. Dirks, H.J. Tanke, G.J. Fleuren, E. Schuuring, A.K. Raap, A novel strategy for human papillomavirus detection and genotyping with SYBR Green and molecular beacon polymerase chain reaction, Am. J. Pathol. 159 (2001) 1651–1660.
[7] I. Nazarenko, B. Lowe, M. Darfler, P. Ikonomi, D. Schuster, A. Rashtchian, Multiplex quantitative PCR using self-quenched primers labeled with a single fluorophore, Nucleic Acids Res. 30 (2002) e37.
[8] Y.S. Lie, C.J. Petropoulos, Advances in quantitative PCR technology: 5′ nuclease assays, Curr. Opin. Biotechnol. 9 (1998) 43–48.
[9] E. Barragan, P. Bolufer, I. Moreno, G. Martin, J. Nomdedeu, S. Brunet, P. Fernandez, C. Rivas, M.A. Sanz, Quantitative detection of AML1–ETO rearrangement by real-time RT–PCR using fluorescently labeled probes, Leuk. Lymphoma 42 (2001) 747–756.
[10] J. Vandesompele, A. De Paepe, F. Speleman, Elimination of primer–dimer artifacts and genomic coamplification using a two-step SYBR Green I real-time RT–PCR, Anal. Biochem. 303 (2002) 95–98.
[11] K.P. Mouillesseaux, K.R. Klimpel, A.K. Dhar, Improvement in the specificity and sensitivity of detection for the Taura syndrome virus and yellow head virus of penaeid shrimp by increasing the amplicon size in SYBR Green real-time RT–PCR, J. Virol. Methods 111 (2003) 121–127.
[12] S.A.E. Marras, F.R. Kramer, S. Tyagi, Multiplex detection of single-nucleotide variations using molecular beacons, Genet. Anal. Biomol. E 14 (1999) 151–156.
[13] G. Breen, D. Harold, S. Ralston, D. Shaw, D.St. Clair, Determining SNP allele frequencies in DNA pools, BioTechniques 28 (2000) 464–470.
[14] S.R. Lewin, M. Vesanen, L. Kostrikis, A. Hurley, M. Duran, L. Zhang, D.D. Ho, M. Markowitz, Use of real-time PCR and molecular beacons to detect virus replication in human immunodeficiency virus type 1-infected individuals on prolonged effective antiretroviral therapy, J. Virol. 73 (1999) 6099–6103.
[15] K. Szuhai, J. Ouweland, R. Dirks, M. Lemaitre, J. Truffert, G. Janssen, H. Tanke, E. Holme, J. Maassen, A. Raap, Simultaneous A8344G heteroplasmy and mitochondrial DNA copy number quantitation in myoclonus epilepsy and ragged-red fibers (MERRF) syndrome by a multiplex molecular beacon based real-time fluorescence PCR, Nucleic Acids Res. 29 (2001) e13.
[16] C. Eckert, O. Landt, T. Taube, K. Seeger, B. Beyermann, J. Proba, G. Henze, Potential of LightCycler technology for quantification of minimal residual disease in childhood acute lymphoblastic leukemia, Leukemia 14 (2000) 316–323.
[17] A. Tsourkas, M.A. Behlke, G. Bao, Structure–function relationships of shared-stem and conventional molecular beacons, Nucleic Acids Res. 30 (2002) 4208–4215.
[18] L.Y. Bustamante, A. Crooke, J. Martínez, A. Díez, J.M. Bautista, Dual-function stem molecular beacons to assess mRNA expression in AT-rich transcripts of *Plasmodium falciparum*, BioTechniques 36 (2004) 488–494.
[19] K.A. Browne, Sequence-specific, self-reporting hairpin inversion probes, J. Am. Chem. Soc. 127 (2005) 1989–1994.
[20] D-M. Kong, L. Gu, H-X. Shen, H-F. Mi, A modified molecular beacon combining the properties of TaqMan probe, Chem. Commun. 8 (2002) 854–855.
[21] M. Zuker, Mfold Web server for nucleic acid folding and hybridization prediction, Nucleic Acids Res. 31 (2003) 3406–3415.
[22] B. Mullah, A. Andrus, Automated synthesis of double dye-labeled oligonucleotides using tetramethylrhodamine (TAMRA) solid supports, Tetrahedron Lett. 38 (1997) 5751–5754.
[23] W.P.C. Stemmer, A. Crameri, K.D. Ha, T.M. Brennan, H.L. Heyneker, Single-step assembly of a gene and entire plasmid from large numbers of oligodeoxyribonucleotides, Gene 164 (1995) 49–53.
[24] F.M. Ausubel, R. Brent, R.E. Kingston, D.D. Moore, J.G. Seidman, J.A. Smith, K. Struhl (Eds.), Short Protocols in Molecular Biology, third ed., John Wiley, New York, 1997.
[25] S.F. Altschul, T.L. Madden, A.A. Schaffer, J. Zhang, Z. Zhang, W. Miller, D.J. Lipman, Gapped BLAST and PSI-BLAST: a new generation of protein database search programs, Nucleic Acids Res. 25 (1997) 3389–3402.
[26] N. Klonis, A.H.A. Clayton, E.W. Voss, W.H. Sawyer, Spectral properties of fluorescein in solvent–water mixtures: applications as a probe of hydrogen bonding environments in biological systems, Photochem. Photobiol. 67 (1998) 500–510.
[27] G.K. Turner, An absolute spectrofluorimeter, Science 146 (1964) 183–189.
[28] J.E. Noble, L. Wang, K.D. Cole, A.K. Gaigalas, The effect of overhanging nucleotides on fluorescence properties of hybridizing oligonucleotides labeled with Alexa-488 and FAM fluorophores, Biophys. Chem. 113 (2005) 255–263.
[29] I. Nazarenko, R. Pires, B. Lowe, M. Obaidy, A. Rashtchian, Effect of primary and secondary structure of oligodeoxyribonucleotides on the fluorescent properties of conjugated dyes, Nucleic Acids Res. 30 (2002) 2089–2095.
[30] A.O. Crockett, C.T. Wittwer, Fluorescein-labeled oligonucleotides for real-time PCR: using the inherent quenching of deoxyguanosine nucleotides, Anal. Biochem. 290 (2001) 89–97.